Analysis of a novel rotating disk cylinder engine concept for power generation

W.G. Le Roux[a]*

P.J. Swanepoel[b]

[a]Department of Mechanical and Aeronautical Engineering,

University of Pretoria, South Africa

[b]Independent Researcher

*Corresponding Author:

Address: Private Bag X20, Hatfield, Pretoria 0028, South Africa

E-mail: willem.leroux@up.ac.za

Summary

A new type of engine concept is proposed, namely a rotating disk cylinder engine. Unique secondary rotors with grooves act as guide vanes for a working fluid to power a main rotor with multiple cylindrical pistons. Currently, no literature exists on the proposed device and the modelling thereof. The aim of this paper is to determine the dynamic and thermodynamic behaviour of the machine so that recommendations can be made for further research work. A transient as well as a steady-state thermodynamic model is developed for an adiabatic expansion process using first and second law analysis with air as ideal gas. The model is compared with experimental results of a piston engine driven by compressed air. Results show that the secondary rotor's angle of rotation is not a linear function of the main rotor's angle of rotation, which suggests a limitation in terms of operating speed. Furthermore, for constant power, the efficiency increases as the inlet pressure and speed decreases, while for constant efficiency, the power increases as the inlet pressure and speed increases. Results show the advantage of using three secondary rotors as it drastically decreases the pressure requirement for a constant torque output. The speed and inlet pressure of the device is, however, limited by the mass and material properties of the rotors as well as the effects of leakage. These limitations have not been considered in this initial analysis of the device and are recommended for future work.

KEY WORDS:

rotating cylinder engine, rotary vane expander, dynamic analysis, thermodynamic analysis, expander, exergy analysis

1 INTRODUCTION

Power generation from steam has become a necessity for everyday life. In recent years, there has been more focus on steam power generation from sustainable heat sources because of fossil fuel depletion [1,2]. Compressed air can also be applied as a green energy source for power generation [3] as well as transportation [4]. To convert fluid energy into mechanical energy, expansion devices are necessary. In terms of renewable energy, expanders are often used in applications such as low-grade heat and waste heat recovery [5-7], compressed-air energy storage [8,9] and solar power generation [10,11]. Expanders can be categorised as velocity or volumetric type [12]. Volumetric expanders can be further categorised as scroll expanders [13-16], screw expanders [17-21], reciprocating piston expanders [22] and vane expanders [12,23,24]. Bao and Zhao [12] did a review of expansion machines and found that the advantages of vane expanders are simplicity, ease of manufacturing and lower costs. Other advantages include low speeds, the possibility of using liquids and wet vapors as working fluid, and low maintenance [12]. According to Imran et al. [23], vane expanders can be further classified into rotary vane expanders [25,26] and revolving vane expanders [27], where the cylinder rotates with the rotor, reducing friction. According to Subiantoro et al. [27], rotary engines are usually more compact and have better noise characteristics and fewer components in comparison with reciprocating engines.

An internal combustion engine, where cylinders are arranged in a radial configuration and the crankshaft remains stationary in operation, is also referred to as a rotary engine. Furthermore, other rotary engine examples include the Wankel engine [28] and “cat-and-mouse type” rotary engine [29]. New methods of converting fluid energy into mechanical energy as well as new engine concepts are often proposed and analysed in literature [29-33]. To continue making improvements in the sustainability, efficiency and cost of generating power, new design concepts have to be evaluated frequently.

A new type of engine concept is introduced and analysed in this paper, namely a rotating disk cylinder engine [34]. The proposed machine can be applied for power generation as an expansion device using compressed air. The proposed device has some similarities with rotating vane expanders and can have the same advantages as were listed above. Figure 1 shows a representation of the proposed machine concept. The main rotor is shown with a smaller secondary rotor, and both rotors are mounted on bearings. Two metallic disks are

used for the main rotor, which is connected to a generator in the case of electric power generation. The metallic disks also act as a flywheel for stability. The fittings between the disks are cylindrical pistons which can move in and out of the grooves of the secondary rotor. The compressed steam or air is fed through the shaft of the secondary rotor and controlled by valves [35,36]. Up to four secondary rotors can be used simultaneously. The device is different from other rotary engines as the unique secondary rotors act as guide vanes for maximum torque on the main rotor. The expansion volume is determined by the diameter and length of the cylindrical pistons. The proposed device can also be used for gas compression, as a hydraulic pump, or for both compression and expansion as in an internal combustion engine [37]. Furthermore, the device can be applied as a compressor/expander unit in a heat pump [38].

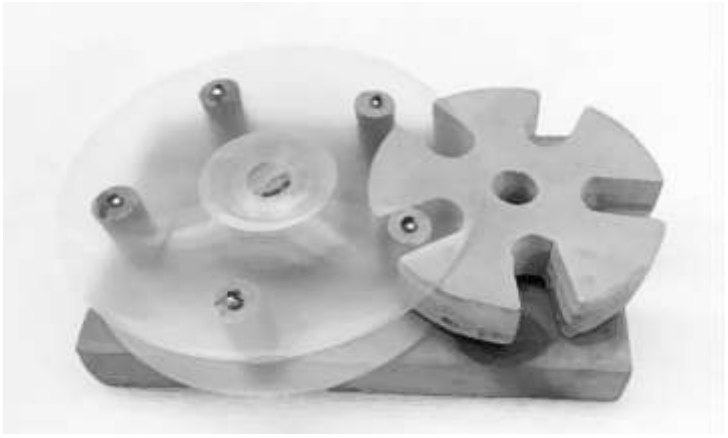

FIGURE 1 An example of the novel rotating disk cylinder engine concept.

According to Subiantoro et al. [27], leakage can be one of the main issues for rotary engines, while lubrication and sealing are listed as disadvantages according to Bao and Zhao [12]. Leakage is also a relevant issue for other volumetric expanders [18,39-43]. Other thermodynamic irreversibilities related to volumetric expanders include inlet and discharge dynamics [40], heat losses [41], oil-flooded mixing [41] and filling [42,43]. The presence of incorrect inlet pressures being supplied creates undesirable effects in a helical screw expander, called blowdown and blowback, which results in loss of work production [17]. Exergy analysis is often applied to determine the performance of a system [22], but it can also be applied in the form of entropy generation minimisation [44]. Subiantoro et al. [27] applied exergy analysis to a revolving vane compressed air engine. The study found that the second-law efficiency decreased with higher operating speed and higher cylinder inertia. Xinghua et al. [8] found that there is small deviation between the real expansion process of a

scroll expander and the ideal isentropic process, which excludes the effects of intake and discharge losses as well as gas leakage.

In this paper, it is assumed that the proposed rotating disk cylinder engine acting as an expansion device has some similarities with a scroll expander [8] and a compressed-air driven piston engine [4]. The authors could not find an expander or engine in the literature that is exactly similar to the proposed device, and therefore a simple dynamic and thermodynamic analysis of the proposed device is presented so that further research can be done. The proposed machine is modelled without leakage and heat loss to predict its performance with air as working fluid. The device is evaluated in terms of isentropic efficiency and recommendations are made for further research work.

2 MODELLING

The rotating disk cylinder engine is modelled as an expansion device for power generation using compressed air. The dynamic modelling of the device is done first, after which a vector analysis and thermodynamic model is presented. A transient model as well as a steady-state model of an adiabatic expansion process is considered.

2.1 Dynamic modelling

Figure 2 shows an example of the machine with a single main rotor and three secondary rotors. As shown in Figure 2, R is the distance between the centre of the main rotor and the centre of the fittings (cylindrical pistons) of the main rotor. The machine is designed so that R is also the radius of the secondary rotors [34]. The main rotor is designed in such a way that its minimum radius is $1.4035R$ and the maximum diameter of the cylindrical pistons is $r = 0.345R$ [34]. A is the distance from the centre of the main rotor to the centre of a secondary rotor. By considering the specific position of the cylindrical piston shown next to the control volume in Figure 2, the distance, A, can be determined with the cosine rule as $A = 2R\cos(36)$. B is the distance from the centre of a secondary rotor to the centre of the end-point of a cylindrical piston so that $B = A - R$. The angle of anti-clockwise rotation of the main rotor is defined as α, while β is the accompanying clockwise angle of rotation of the secondary rotor. L denotes the distance from the centre of the main rotor to the line in which direction the force of the cylindrical piston is acting. L is defined as shown in Eq. (1), where β is found using Eq. (2). The angular velocity and angular acceleration of a secondary rotor is shown in Eq. (3) and Eq. (4), respectively.

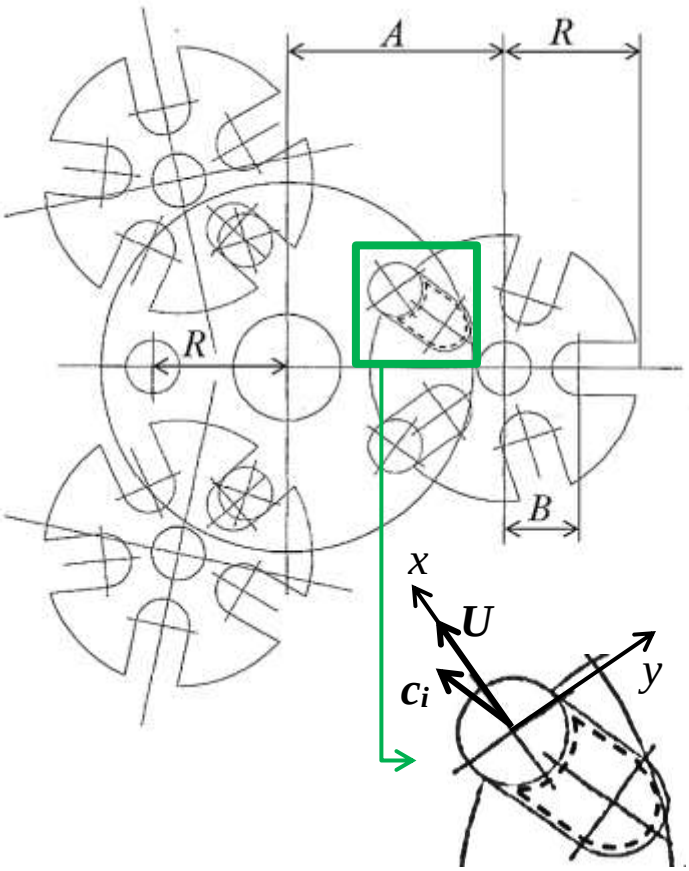

FIGURE 2 The rotating disk cylinder engine with main rotor and three secondary rotors (with control volume and velocities indicated).

$$L/R = \mathrm{A}\sin(\beta)/R \tag{1}$$

$$\beta = \arctan\left(\frac{\sin(\Omega t)}{A/R - \cos(\Omega t)}\right) \tag{2}$$

$$\omega = \frac{d\beta}{dt} = \Omega\left[\frac{(A/R)\cos\alpha - 1}{(A/R)^2 - 2(A/R)\cos\alpha + 1}\right] \tag{3}$$

$$\varphi = \frac{d\beta''}{dt} = \Omega^2\left[\frac{\left((A/R) - (A/R)^3\right)\sin\alpha}{\left((A/R)^2 - 2(A/R)\cos\alpha + 1\right)^2}\right] \tag{4}$$

The incremental volume is defined in Eq. (5), where *d* is the inner width of the main rotor, as well as the length of the cylindrical pistons, and thickness of the secondary rotors. S_2 is the distance between the centre of the secondary rotor and the cylindrical piston, where

$S_2 = S - S_1 = \sqrt{A^2 - L^2} - \sqrt{R^2 - L^2}$. S is the distance between a main rotor and a secondary rotor using a straight line through the cylindrical piston and the secondary rotor centre.

$$\Delta V = \frac{\pi}{2} dr \Delta S_2 \tag{5}$$

2.2 Vector analysis

From Figure 2, the relative inlet velocity of air, w_i, can be calculated with Eq. (6), since $w_i^2 = w_{i,x}^2 + c_{i,y}^2$ and $U = \Omega R$. Note that $w_i^2 = U^2 + c_i^2$ when $\alpha = \beta = 0^\circ$. Furthermore, the absolute inlet velocity can be calculated as $c_i = \dot{m} / \rho_i A_i$. The relative inlet velocity, w_i, is used in the thermodynamic modelling of the proposed rotating disk cylinder engine.

$$w_i = \sqrt{(\Omega R - c_i \sin(\alpha + \beta))^2 + (c_i \cos(\alpha + \beta))^2} \tag{6}$$

2.3 Thermodynamic modelling

2.3.1 Transient model

An adiabatic control volume boundary around the working fluid on the inside of the expansion groove is considered, as shown in Figure 2. To solve the required pressure, temperature and mass of the working fluid as a function of α, an ideal gas thermodynamic analysis is performed, similar to Xinghua et al. [8]. The input constants are P_i, T_i, $\dot{W}_L$ and Ω. For each time step of α, ΔV and P_R are calculated using Eq. (5) and Eq. (7), respectively.

$$\dot{W}_L = \tau\Omega = FL\Omega = \frac{\pi}{2} P_R dr L \Omega \tag{7}$$

The work produced, as a function of α, is $W = \int P dV$, where $P = P_R + P_0$. The mass on the inside of the control volume, m_2, per time step of α, is assumed so that T_2 can be calculated using the ideal gas equation. According to the first law of thermodynamics, m_2 can be calculated as shown in Eq. (8), where $m_i = m_2 - m_1$. The mass is calculated in an iterative process.

$$m_2 = \frac{W + P_2 V_2 c_{v0} / \gamma + m_1 \gamma T_i + m_1 c_{v0} (T_i - T_1) + m_1 w_i^{\,2} / 2}{c_{v0} T_i + \gamma T_i + w_i^{\,2} / 2} \tag{8}$$

For the outlet at P_0, a control mass boundary around the air is used so that the outlet volume can be calculated as shown in Eq. (9).

$$V_2 = \frac{m_1 c_{v0} T_1 + P_0 V_1}{P_0 + P_2 c_{v0} / \gamma} \tag{9}$$

2.3.2 Steady-state model

The actual outlet temperature, T_e, is calculated with Eq. (10), using the first law and assuming no heat loss. An average mass flow rate is used as calculated from Section 2.3.1 in an iterative process.

$$T_e = T_i + \frac{0.5\dot{m}\left(c_i^{\,2} - c_e^{\,2}\right) - \dot{W}}{\dot{m} c_p} \tag{10}$$

$$c_e = \frac{\dot{m} \gamma T_e}{P_e dr} \tag{11}$$

The outlet velocity is calculated with Eq. (11). Eq. (10) and Eq. (11) are solved simultaneously to determine c_e and T_e. The performance of the expander can be expressed in terms of isentropic efficiency [21]. The efficiency is calculated as shown in Eq. (12).

$$\eta_s = \frac{T_i - T_{es}}{T_i - T_e} = \frac{T_i \left(1 - \left(P_e / P_i\right)^{\frac{k-1}{k}}\right)}{\left[\dot{W} - 0.5\dot{m}\left(c_i^{\,2} - c_e^{\,2}\right)\right] / \dot{m} c_p} \tag{12}$$

The efficiency can also be calculated as $\eta_s = (\dot{\Psi} - \dot{I}) / \dot{\Psi}$, where $\dot{I} = T_a \dot{S}_{gen} = \dot{\Psi} - \dot{W}$. The entropy generation rate is calculated with Eq. (13) and the exergy transfer by flow is calculated using Eq. (14).

$$\dot{S}_{gen} = \dot{m}\left(s_e - s_i\right) = \dot{m} c_{p0} \ln\left(\frac{T_e}{T_i}\right) - \dot{m} \gamma \ln\left(\frac{P_e}{P_i}\right) > 0 \tag{13}$$

$$\dot{\Psi} = \dot{m}\left(\psi_i - \psi_e\right) = \dot{m}\left[h_i - h_e - T_a\left(s_i - s_e\right) + \frac{\left(c_i^{\,2} - c_e^{\,2}\right)}{2} \right] \tag{14}$$

3 RESULTS AND DISCUSSION

3.1 Dynamic behaviour

Figure 3 shows the angle of rotation of each of the three secondary rotors as a function of the main rotor's angle of rotation, according to Eq. (2). Results show that the rotation of the secondary rotors is not a linear function of the main rotor's angle of rotation. The rotation of a secondary rotor is thus not similar to the rotation of the main rotor, except when β is close to 0˚. The angular velocity of the secondary rotor increases as the main rotor's cylindrical piston moves into the groove of the secondary rotor. The angular acceleration becomes negative as the cylindrical piston leaves the groove of the secondary rotor. As the next cylindrical piston slides into the secondary rotor, a spike in angular acceleration takes place. These results suggest that there exists a limiting factor in terms of the operating speed of the device. Furthermore, Figure 4 shows the dimensionless length (L/R) at which the fluid is acting onto the main rotor in the case of power generation, according to Eq. (1). To sustain the rotation, a force is applied to the main rotor at intervals of 24˚.

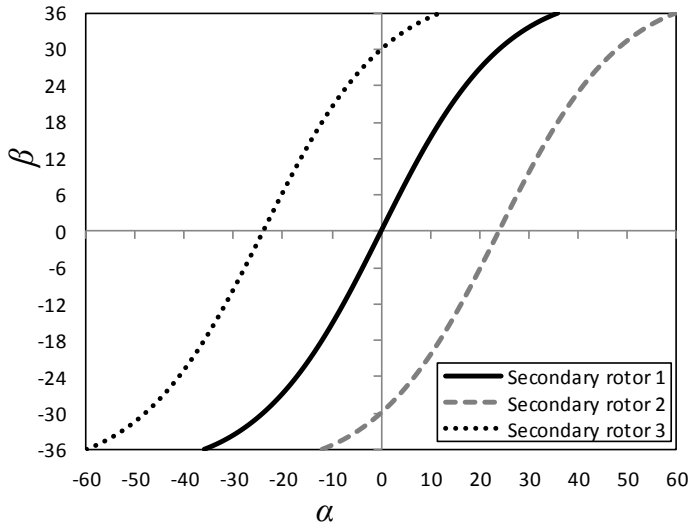

FIGURE 3 Angle of rotation of the secondary rotors as a function of the angle of rotation of the main rotor.

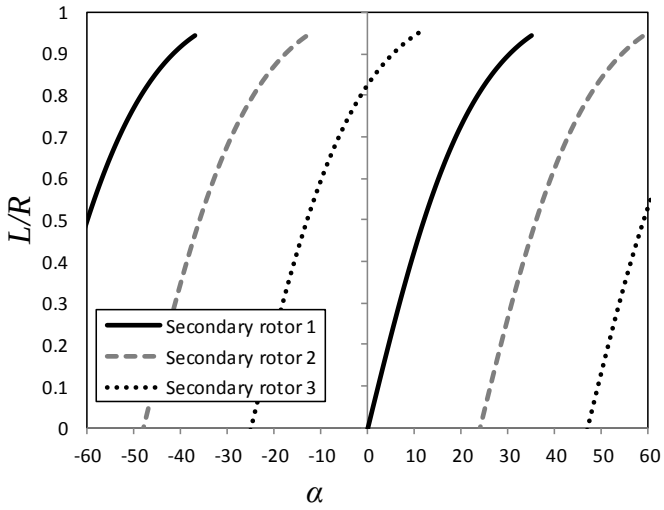

FIGURE 4 Radius at which the force of expanding gas is acting onto the main rotor.

3.2 Thermodynamic behaviour

3.2.1 Comparison with experimental work

Results have been compared with experimental work done by Huang et al. [4], in which a 100 cm^3 piston engine was driven by compressed air. Table 1 shows the measured output power, rotational speed and inlet temperature for three different cases of the piston engine operating at an inlet pressure of 9 bar (absolute). These input parameters have been used in the thermodynamic model and the results of the model are also shown in Table 1. The simulation results compare well with the experimental results as the largest percentage difference is 14.5%. According to Huang et al. [4], the energy conversion efficiency is $\eta_{EC} = \tau\Omega / P_i Q$.

Note that the default constants used in the analysis were A_i = 0.0003 m^2, c_{p0} = 1004 J/kgK, γ = 287 J/kgK, d = 0.0397 m, P_e = 86 kPa, R = 0.115 m and r = 0.0345 m. Table 1 also shows additional simulation results for each of the three cases considered. Note that the load and speed adjustment, and therefore a torque adjustment, does have an effect on the average mass flow rate, outlet temperature and the isentropic efficiency. Results show that, for a constant inlet pressure, the isentropic efficiency decreases as the angular velocity of the main rotor increases. This result was also found by Subiantoro et al. [27].

TABLE 1 Comparison with experimental work by [4] for inlet pressure of 9 bar.

Case	**1**		**2**		**3**	
Ω (rpm)	500		750		1000	
T_i (K)	309		309		310	
$\dot{W}_L$ (W)	500		710		850	
	Exp.	**Model**	**Exp.**	**Model**	**Exp.**	**Model**
τ (Nm)	10	9.55	8.85	9.04	7.85	8.12
T_e (K)	258	266	260	268	264	272
Q (l/min)	550	534	760	802	960	1069
η_{EC} (%)	6.75	6.24	6.9	5.9	6.2	5.3
U (m/s)		6.02		9.03		12.0
$\dot{m}$ (kg/s)		0.0123		0.0181		0.0233
η_s (%)		26.8		25.8		23.9
$\dot{S}_{gen}$ (W/K)		6.52		9.72		12.8
$\dot{\Psi}$ (W)		2456		3627		3835

3.2.2 Pressure requirement

Figure 5 shows the required pressure on a cylindrical piston of the main rotor to overcome the constant power load of 500 W at 500 rpm (see Table 1) if a single secondary rotor is considered. It should be noted that for a single secondary rotor, the pressure requirement is initially very high due to the initial small torque radius, *L*, as shown in Figure 4. However, the overlapping of the contact times of all three secondary rotors should be considered. According to Figure 5, when α is between 0˚ and 12˚ for Secondary Rotor 1, a much smaller pressure is necessary to sustain the power load if Secondary Rotor 2 is used. The large pressure at Secondary Rotor 1 is thus not required. The overlapping of the secondary rotors means that effectively, a force is applied to the main rotor at intervals of 24˚ of rotation to sustain the rotation, as also shown in Figure 4.

Figure 6 shows the effect of overlapping of the secondary rotors. The pressure requirement becomes relatively constant and is drastically reduced. Note that the pressure requirement is still initially larger when α = 12˚ for the first secondary rotor as it takes over the load from the previous rotor. It is thus assumed that there is no load on the first secondary rotor until α is at 12˚.

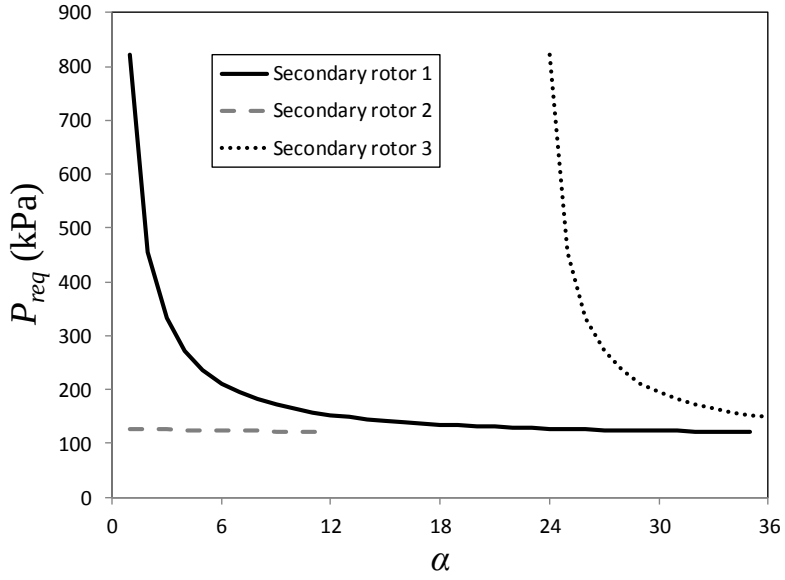

FIGURE 5 Overlapping of the pressure requirement on the main rotor for a constant power of 500 W at 500 rpm.

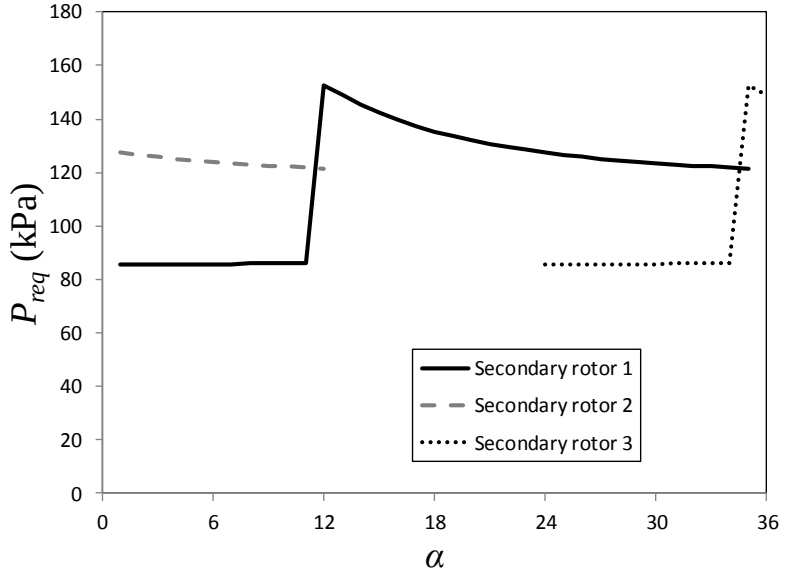

FIGURE 6 The required pressure in the groove of each secondary rotor for a constant power of 500 W at 500 rpm, where Secondary Rotor 1 carries the main rotor's load from 12˚ to 36˚.

TABLE 2 Simulation results at 2.5 bar inlet pressure.

Case	**1**	**2**	**3**
T_e (K)	267	269	275
η_{EC} (%)	22.5	21.2	19.1
η_s (%)	49.9	48.1	44.5
$\dot{S}_{gen}$ (W/K)	2.01	3.05	4.16
$\dot{\Psi}$ (W)	1102	1624	2097

The results above show that a much lower inlet pressure is necessary to sustain the main rotor at steady state power. Table 2 therefore shows expected results for an inlet pressure of 2.5 bar instead of 9 bar. Note that the isentropic efficiencies and energy conversion efficiencies in Table 2 are therefore much higher than in Table 1.

Figure 7 shows the required total mass in the groove between the main and secondary rotor, for constant torque (see Table 1). Note that more air is required to sustain a larger torque, as shown in Figure 7, according to Eq. (8). Furthermore, the required timing of the inlet valve for constant power on the main rotor is shown in Figure 8. The inlet valve area as a function of α was determined according to Eq. (15) and Eq. (16), where k = 1.4, C_k = 3.864, C_r = 0.528, C_0 = 0.0404 and $C_D \approx 0.8$ [16,25,35,36]. If $\left(P/P_i\right) \le C_r$ (for choked flow), $f\left(P/P_i\right) = 1$. For $\left(P/P_i\right) > C_r$, Eq. (16) is applied. The sudden increase in required valve inlet area, as shown in Figure 8, is due to the transition from one secondary rotor to another. Note that the results above show the required inlet area for constant torque, which represents an ideal situation.

$$\dot{m} = \frac{C_D C_0 A_i P_i f\left(P/P_i\right)}{\sqrt{T_i}} \tag{15}$$

$$f\left(P/P_i\right) = C_k \left[\left(\frac{P}{P_i}\right)^{2/k} - \left(\frac{P}{P_i}\right)^{(k+1)/k} \right]^{1/2} \tag{16}$$

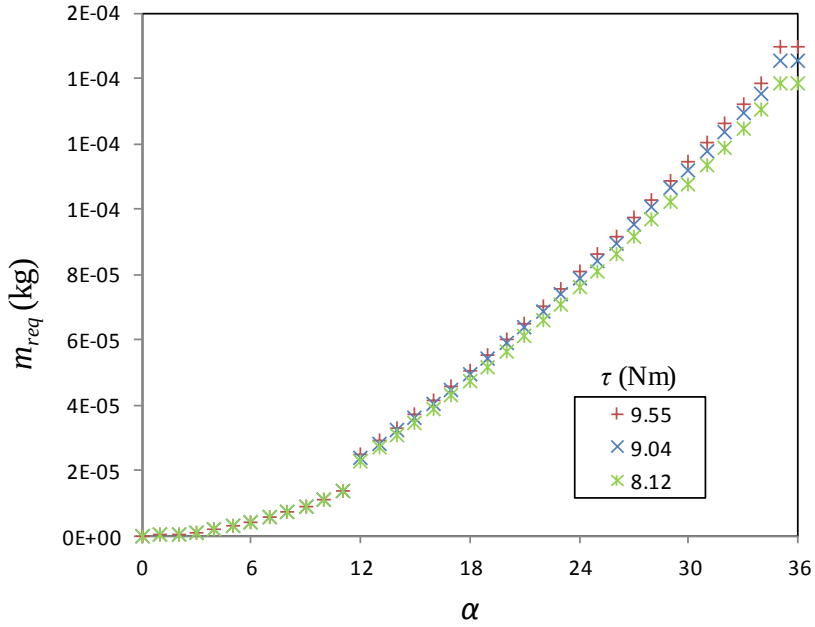

FIGURE 7 Mass of air in the groove as a function of α and torque for an inlet pressure of 2.5 bar.

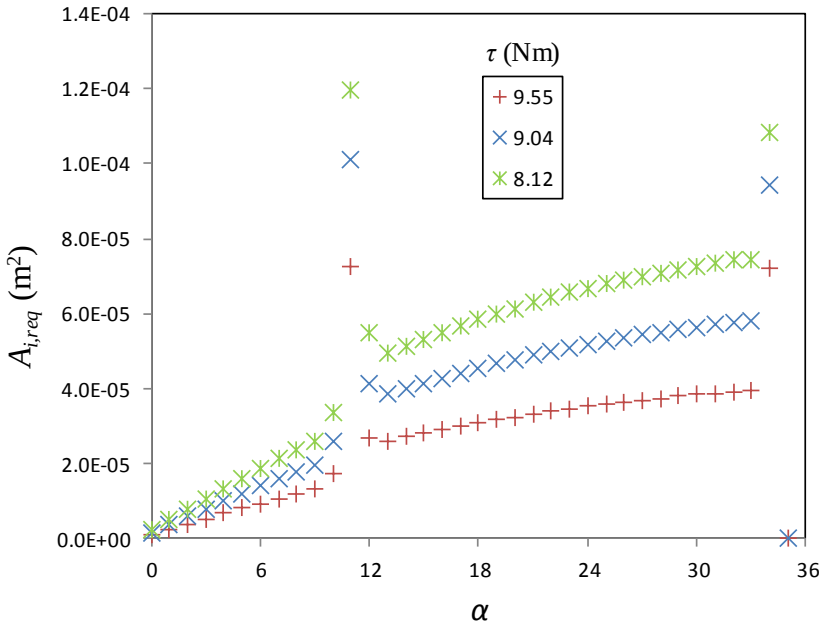

FIGURE 8 Valve timing for constant torque as a function of α, for an inlet pressure of 2.5 bar.

The results in this section show the required conditions for a constant power output. However, in practice, the power output would be a function of α. The results given are therefore an initial investigation which can be used for design purposes. Further numerical and experimental analysis is recommended, especially in terms of matching the inlet pressure with the angular velocity. It should be further noted that, in this initial investigation, it was assumed that no leakage takes place and that no compression takes place at other rotor

positions which could resist the rotation of the main rotor. These effects are also recommended for further work, where the combined compression and expansion stages can be investigated for use in a heat engine.

3.2.3 Efficiency analysis

Results show that, for a constant torque, the efficiency increases when the inlet pressure decreases, as shown in Figure 9. Figure 9 also shows that the efficiency increases as the torque increases for a constant inlet pressure. Furthermore, the results from Figure 9 show that, for a constant efficiency, the torque increases as the inlet pressure increases. For a constant efficiency, a larger power load could thus be sustained at higher speed and inlet pressure. These results (as well as the results in Table 1) suggest that for maximum power, a high speed and high inlet pressure would be required, as was also found for single screw expanders with air as working fluid, and for twin-screw expanders used in organic Rankine cycles [19,20]. It should also be noted that the speed of the main rotor will depend on the inlet pressure and mass of the rotor. The speed and inlet pressure of the rotor are, however, limited by the mass and material properties of the rotors as well as vibrations and pressure wave propagations [4]. These limitations were not further considered in this initial analysis of the device, but are recommended for future work. The rotors should be designed in such a way that the selected pressure ratio is a compromise between the efficiency and power output at steady state.

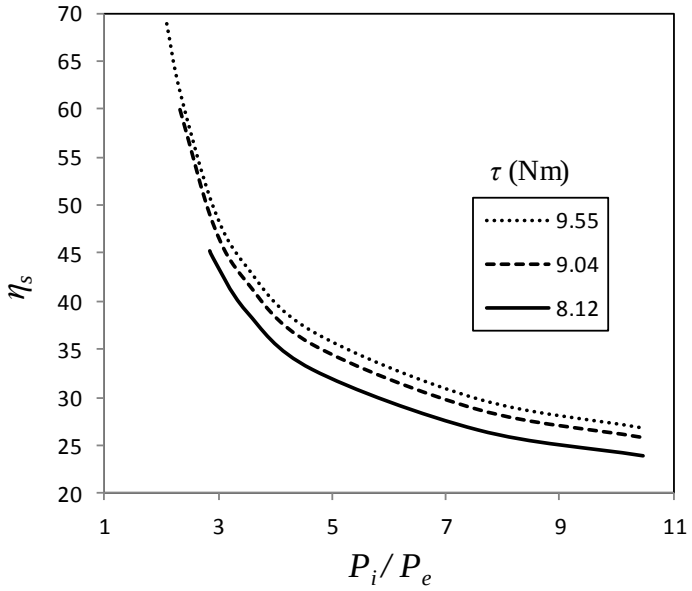

FIGURE 9 Effect of pressure ratio on the exergetic performance of the device.

4 CONCLUSION AND RECOMMENDATIONS

A new type of engine concept was proposed, namely a rotating disk cylinder engine. Secondary rotors with grooves act as guide vanes for the working fluid to power a main rotor. The proposed engine can be applied in the conversion of renewable energy sources for power generation and has potential for low costs in terms of manufacturing. Currently, no literature exists on the proposed device and the modelling thereof. The aim of this paper was to determine the dynamic and thermodynamic behaviour of the machine so that recommendations can be made for further research work. A transient as well as a steady-state thermodynamic model was developed for an adiabatic expansion process using first and second law analysis with air as ideal gas. It was assumed that there is no leakage and that no compression takes place at other rotor positions which could resist the rotation of the main rotor. The model was compared with experimental results of a piston engine running at speeds of between 500 rpm and 1000 rpm, power output of between 500 W and 850 W, and driven by compressed air at 9 bar. The results compared well, with the largest difference being 14.5%. Results from the thermodynamic analysis showed that for maximum power at constant efficiency, a high speed and high pressure ratio would be required, but for maximum efficiency at constant power, a lower pressure ratio and speed is required. The results from the dynamic analysis showed that the rotation angle of the secondary rotor is not a linear function of the main rotor's angle of rotation, which suggests a limiting factor in terms of the operating speed of the device. Furthermore, results showed that three secondary rotors significantly decrease the pressure requirement if a constant torque output is sought. The device therefore has potential for high efficiencies in low pressure and low speed applications. Further work is recommended, especially in terms of matching the inlet pressure with the angular velocity. It is recommended that the device should be tested in an experimental setup so that further improvements and innovations on the concept can be developed.

NOMENCLATURE

A	distance between centre of main rotor and centre of secondary rotor (m)
A_i	inlet area (m^2)
B	distance between centre of secondary rotor and centre of groove end-point (m)
c	absolute velocity (m/s)
c_{p0}	specific heat at constant pressure (J/kgK)
c_{v0}	specific heat at constant volume (J/kgK)
d	distance between the two disks that form the main rotor (m)
F	force (N)
g	gravitational acceleration (m/s^2)
h	specific enthalpy (kJ/kg)
$\dot{I}$	irreversibility rate
k	ratio of specific heats
L	distance from centre of main rotor to the line in which direction the force of cylindrical piston is acting (m)
m	mass (kg)
$\dot{m}$	mass flow rate (kg/s)
P	pressure (kPa)
Q	volumetric flow rate (m^3/s)
$\dot{Q}$	heat transfer rate (W)
r	diameter of the cylindrical piston (m)
R	distance between centre of main rotor and centre of cylindrical piston (m)
s	specific entropy (kJ/kgK)
S	distance between rotors using a straight line through cylindrical piston and secondary rotor (m)
S_1	distance between main rotor and cylindrical piston in the direction of the force of the cylindrical piston (m)
S_2	distance between secondary rotor and cylindrical piston (m)
$\dot{S}_{gen}$	entropy generation rate (W/K)
t	time (s)
T	temperature (K)
U	cylindrical piston velocity (m/s)
V	volume (m^3)

w relative velocity (m/s)

W work (J)

$\dot{W}$ power (W)

z height (m)

Greek symbols

α angle of rotation of the main rotor

β angle of rotation of a secondary rotor

γ ideal gas constant (J/kgK)

η efficiency

ρ density (kg/m^3)

τ torque (Nm)

$\dot{\Psi}$ exergy rate (W)

ψ specific exergy (J/kg)

φ angular acceleration of secondary rotor (rad/s^2)

Ω angular velocity of main rotor (rad/s)

ω angular velocity of secondary rotor (rad/s)

Subscripts

0 stagnation

1 at state 1

2 at state 2

a atmospheric

d dynamic

e exit

EC energy conversion

i inlet

L load

req required

R resultant

s isentropic

x in the x-direction

REFERENCES

1. Subramani L, Parthasarathy M, Balasubramanian D, Ramalingam K. Novel Garcinia gummi-gutta Methyl Ester (GGME) as a potential alternative feedstock for existing unmodified DI diesel engine. *Renewable Energy* 2018; **125**:568–577.

2. Balasubramanian D, Arumugam SRS, Subramani L, Chellakumar IJLJS, Mani A. A numerical study on the effect of various combustion bowl parameters on the performance, combustion, and emission behavior on a single cylinder diesel engine. *Environmental Science and Pollution Research* 2018; **25**(3):2273–2284.

3. Milewski J, Badyda K, Szabłowski L. Compressed air energy storage systems. *Journal of Power Technologies* 2016; **96**(4):245–260.

4. Huang C, Hu C, Yu C, Sung C. Experimental investigation on the performance of a compressed-air driven piston engine. *Energies* 2013; **6**:1731–1745.

5. Lemort V, Quoilin S, Cuevas C, Lebrun J. Testing and modeling a scroll expander integrated into an Organic Rankine Cycle. *Applied Thermal Engineering* 2009; **29**:3094-3102.

6. Amiri Rad E, Mohammadi S. Energetic and exergetic optimized Rankine cycle for waste heat recovery in a cement factory. *Applied Thermal Engineering* 2018; **132**:410–422.

7. Minea V. Power generation with ORC machines using low-grade waste heat or renewable energy. *Applied Thermal Engineering* 2014; **69**:143–154.

8. Xinghua Y, Jiazhen P, Jidai W, Jing S. Simulation and experimental research on energy conversion efficiency of scroll expander for micro-Compressed Air Energy Storage system. *International Journal of Energy Research* 2014; **38**:884–895.

9. Najjar YSH, Abubaker AM. Using novel compressed-air energy storage systems as a green strategy in sustainable power generation–a review. *International Journal of Energy Research* 2016; **40**:1595–1610.

10. Freeman J, Guarracinoa I, Kalogirou SA, Markides CN. A small-scale solar organic Rankine cycle combined heat and power system with integrated thermal energy storage. *Applied Thermal Engineering* 2017; **127**:1543–1554.

11. Le Roux WG, Bello-Ochende T, Meyer JP. Operating conditions of an open and direct solar thermal Brayton cycle with optimised cavity receiver and recuperator. *Energy* 2011; **36**: 6027–6036.

12. Bao J, Zhao L. A review of working fluid and expander selections for organic Rankine cycle. *Renewable and Sustainable Energy Reviews* 2013; **24**:325–342.

13. Kim H, Kim W, Kim H, Kim S. Applicability of scroll expander and compressor to an external power engine: Conceptual design and performance analysis. *International Journal of Energy Research* 2011; **36**:385–396.

14. Li T, Zhu J, Fu W, Hu K. Experimental comparison of R245fa and R245fa/R601a for organic Rankine cycle using scroll expander. *International Journal of Energy Research* 2015; **39**:202–214.

15. Tarique MdA, Dincer I, Zamfirescu C. Experimental investigation of a scroll expander for an organic Rankine cycle. *International Journal of Energy Research* 2014; **38**:1825–1834.

16. Luo X, Wang J, Krupke C, Xu H. Feasibility study of a scroll expander for recycling low-pressure exhaust gas energy from a vehicle gasoline engine system. *Energies* 2016; **9**(4):231.

17. Ng KC, Bong TY, Lim TB. A thermodynamic model for the analysis of screw expander performance. *Heat Recovery Systems & CHP* 1990; **10**(2):119–133.

18. Kaneko T, Hirayama N. Study on fundamental performance of helical screw expander. *Bulletin of Japan Society of Mechanical Engineers (JSME)* 1985; **28**(243):1970–1977.

19. He W, Wu Y, Peng Y, Zhang Y, Ma C, Ma G. Influence of intake pressure on the performance of single screw expander working with compressed air. *Applied Thermal Engineering* 2013; **51**:662–669.

20. Tang H, Wu H, Wang X, Xing Z. Performance study of a twin-screw expander used in a geothermal organic Rankine cycle power generator. *Energy* 2015; **90**:631–642.

21. Ziviania D, Desideri A, Lemort V, De Paepe M, Van den Broek M. Low-order models of a single-screw expander for organic Rankine cycle applications. *IOP Conf. Series: Materials Science and Engineering*, 2015; **90**. Paper 012061.

22. Sayin C, Hosoz M, Canakci M, Kilicaslan I. Energy and exergy analyses of a gasoline engine. *International Journal of Energy Research* 2007; **31**(3):259–273. https://doi.org/10.1002/er.1246.

23. Imran M, Usman M, Park B, Lee D. Volumetric expanders for low grade heat and waste heat recovery applications. *Renewable and Sustainable Energy Reviews* 2016; **57**:1090–1109.

24. Subiantoro A, Tiow OK. Introduction of the revolving vane expander. *HVAC&R Research* 2009; **15**(4):801–816.

25. Luo X, Wang J, Shpanin L, Jia N, Liu G, Zinober ASI. Development of a mathematical model for vane-type air motors with arbitrary N vanes. *Proceedings of the World Congress on Engineering* 2008.

26. Shen Y, Hwang Y. Design and implementation of an air-powered motorcycles. *Applied Energy* 2009; **86**(7-8):1105–1110.

27. Subiantoro A, Wong KK, Ooi KT. Exergy Analysis of the Revolving Vane Compressed Air Engine. *International Journal of Rotating Machinery* 2016; Article ID 5018467.

28. Antonelli M, Baccioli A, Francesconi M, Desideri U, Martorano L. Operating maps of a rotary engine used as an expander for micro-generation with various working fluids. *Applied Energy* 2014. **113**:742–750.

29. Sakita M. A cat-and-mouse type rotary engine: engine design and performance evaluation. *Proceedings of the Institution of Mechanical Engineers*, 2006; **220** Part D, 1139.

30. Ertesvåg IS. Analysis of the Vading concept - a new rotary-piston compressor, expander and engine principle. *Proceedings of the Institution of Mechanical Engineers, Part A: Journal of Power and Energy* 2002; **216**(3):283–290.

31. Korakianitis T, Boruta M, Jerovsek J, Meitner PL. Performance of a single nutating disk engine in the 2 to 500 kW power range. *Applied Energy* 2009; **86**:2213–2221.

32. Cao Y. Theory and performance analysis of a new heat engine for concentrating solar power. *International Journal of Energy Research* 2014; **38**:1812–1824.

33. Daoud JM, Friedrich D. Performance investigation of a novel Franchot engine design. *International Journal of Energy Research* 2018; **42**(2):673–683. https://doi.org/10.1002/er.3850

34. Spoor and Fisher. Internal Combustion Chamber. *Patent Journal of South Africa* 2008; **41**(9) (Part 2, 2):2008/06636.

35. Pu J, Weston RH. Steady state analysis of pneumatic servo drives. *Proc. Instn. Mech. Engrs, Part C: Journal of Mechanical Engineering Science* 1990; **204**:377–387.

36. Lai G et al. Parallel kinematic mechanisms for distributed actuation of future structures. *Journal of Physics: Conference Series* 2016. **744**:012169.

37.Rakopoulos CD. Evaluation of a spark ignition engine cycle using first and second law analysis techniques. *Energy Conversion and Management* 1993; **34**(12):1299–1314.

38. Henderson PC, Hewitt NJ, Mongey B. An economic and technical case for a compressor/expander unit for heat pumps. *International Journal of Energy Research* 2000; **24**:831–842.

39. Read M, Stosic N, Smith IK. Optimization of screw expanders for power recovery from low-grade heat sources. *Energy Technology & Policy* 2014; **1**:131–142.

40. Sangfors B. Analytical modeling of helical screw machine for analysis and performance prediction. *Proceedings of the International Compressor Engineering Conference at Purdue*, 1982. Paper 384.

41. Ziviania D, Van den Broek M, De Paepe M. Geometry-based modeling of single screw expander for organic Rankine cycle systems in low-grade heat recovery. *Energy Procedia* 2014; **61**:100–103.

42. Papes I, Degroote J, Vierendeels J. Analysis of a twin screw expander for ORC systems using computational fluid dynamics with a real gas model. *Proceedings of the International Compressor Engineering Conference in Purdue*, 2014. Paper 2350.

43. Papes I, Degroote J, Vierendeels J. Numerical simulation of a twin screw expander for performance prediction. *IOP Conf. Series: Materials Science and Engineering* 2015; **90**. Paper 012059.

44. Le Roux WG, Bello-Ochende T, Meyer JP. Thermodynamic optimisation of the integrated design of a small-scale solar thermal Brayton cycle. *International Journal of Energy Research* 2012; **36**:1088–1104.